Development and Characterization of Blast Apparatus for Preclinical Auditory and Vestibular Research

Yuan Gao[1], Pavan Krishnan[1], Megan J. Barber[1], Federica M. Raciti[1,2], Curtis S. King[3], Michael E. Hoffer[1] and Suhrud M. Rajguru[1,2,3]

UNIVERSITY OF MIAMI MILLER SCHOOL of MEDICINE

[1]Dept. of Otolaryngology, University of Miami, Miami FL;
[2]Dept. of Biomedical Engineering, University of Miami, Miami FL
[3] RestorEar Devices

UNIVERSITY OF MIAMI COLLEGE of ENGINEERING

INTRODUCTION

Blast injuries pose a major concern affecting approximately 15-20% of deployed military personnel and civilians in high-risk occupations. High-energy shock waves and rapid pressure changes from blasts can cause significant damage to both auditory and vestibular systems, leading to hearing loss, tinnitus, dizziness, vertigo, and balance issues. These injuries carry long-term consequences and impose a substantial financial burden on governments and affected individuals. To facilitate research into blast injury mechanisms and therapeutic interventions, this study focuses on developing a well-characterized blast apparatus that can replicate mild blast conditions within the clinically relevant range of 70-110 kPa (10-15 psi).

METHOD

1 Blast Apparatus Overview

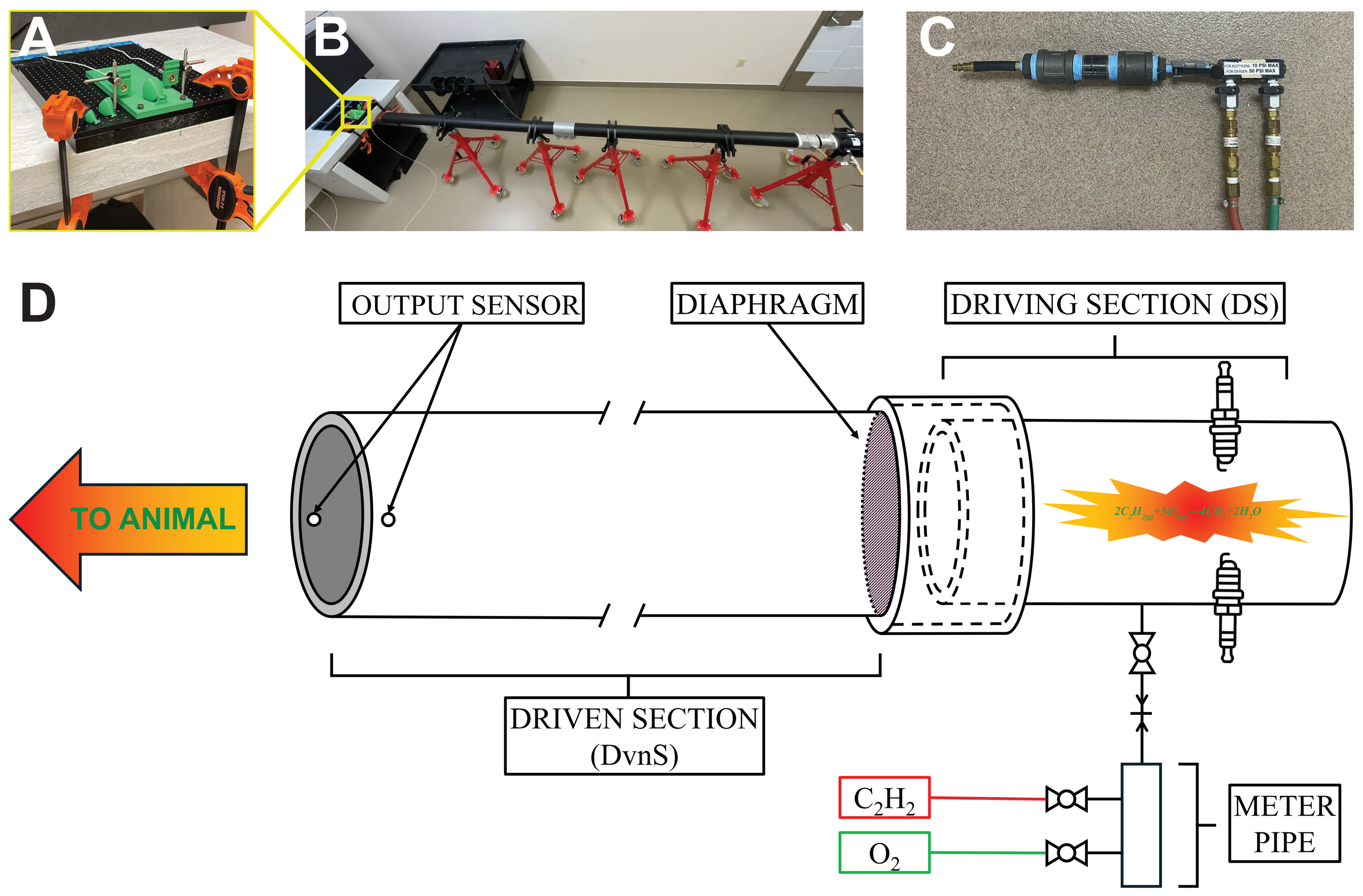

Figure 1. Design and configuration of the oxy-acetylene combustion blast apparatus. A) Close-up of the animal holding platform and ear-sensor mounts located 15 in from the open end of the tube. **B)** Photograph of the complete blast-tube system. **C)** Meter-pipe assembly used to deliver controlled quantities of C_2H_2 and O_2 to the DS. Loading consistency was maintained by fully pressurizing the meter pipe and allowing the pressure to equilibrate between the meter pipe and the DS before closing the valves, ensuring that the same gas quantity was introduced during each loading cycle. **D)** Schematic of the apparatus. The DvnS and DS are separated by a replaceable rupture diaphragm. High-frequency ICP® pressure sensors (PCB Piezotronics, model 113B27) were used to measure the blast-pressure waveforms. The sensors have a measurement range of 100 psi, a sensitivity of 50 mV/psi, a rise time of ≤1 μs, and a resonant frequency of ≥500 kHz. Pressure signals were recorded at a sampling frequency of 10 kHz per channel.

Table 1. Blast Apparatus Component Dimension

Components	Length (mm | inch)	Inner Diameter (mm | inch)	Outer Diameter (mm | inch)
DvnS	3225 | 127.0	77 | 3.0	89 | 3.5
DS	300 | 12.0	77 | 3.0	89 | 3.5
Meter Pipe	177 | 7.0	25 | 1.0	35 | 1.5

Table 2. Environmental Conditions during Blast Experiments

	Temperature	Humidity (%)	Atmospheric Pressure	$P_{C_2H_2}$	P_{O_2}
SI	295.7 ± 2.5 K	77	101.3 ± 1.0 kPa	34.5 kPa	137.9 kPa
Imperial	72.5 ± 4.5 °F		14.7 ± 0.14 psi	5.0 psi	20 psi

2 Operating Procedure

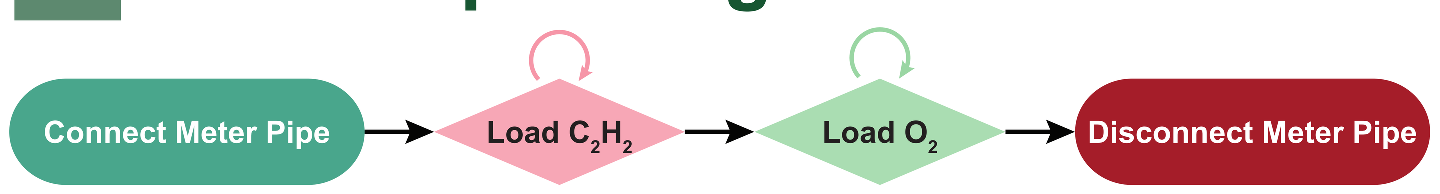

Figure 2. Operating Procedure. Blast intensity can be adjusted using two approaches. First, the working pressures of the acetylene and oxygen cylinders can be changed while maintaining the required gas ratio. Second, intensity can be increased by repeating the loading sequence shown in the diagram. Each loading cycle consists of connecting the meter pipe, loading C_2H_2 followed by O_2, and then disconnecting the meter pipe.

CONCLUSION

The tested apparatus produced controlled and reproducible peak overpressures across different oxy-acetylene working-pressure conditions and loading cycles, demonstrating its ability to generate blast exposures ranging from mild to higher intensities. The apparatus will next be used in animal studies to investigate blast-injury mechanisms and evaluate potential protective or therapeutic interventions. Future work will include establishing a repetitive-blast protocol, expanding the system to model more severe blast conditions, and adapting the platform to study blast effects on additional physiological systems.

RESULTS

3 Apparatus Generated Blast Waveforms Resemble Open-Field Explosion Waveforms

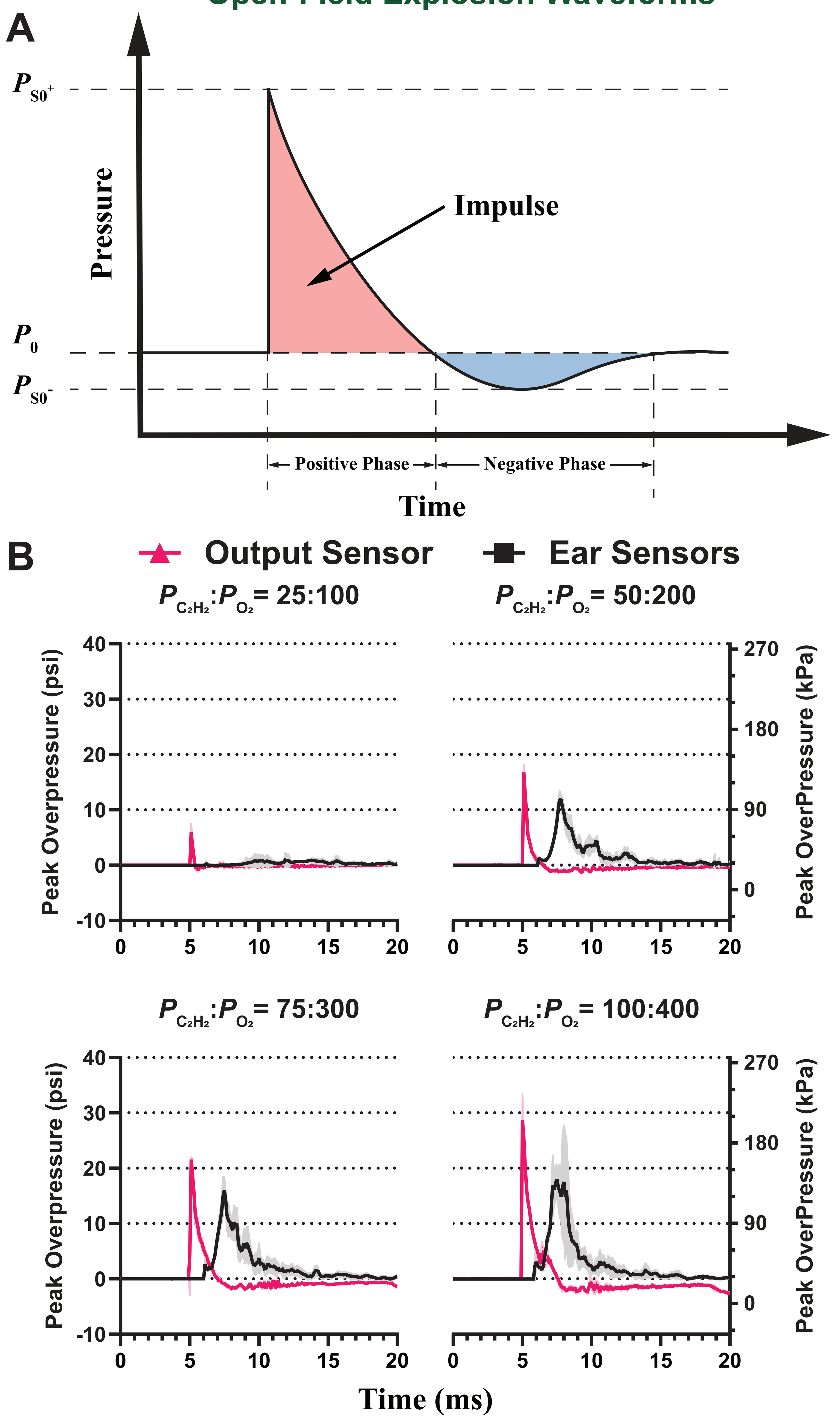

Figure 3. Representative blast-pressure waveforms generated at different acetylene-to-oxygen working pressures. A) Ideal Friedländer waveform, including the rapid pressure rise, exponential decay during the positive phase, and subsequent negative-pressure phase. **B)** Representative pressure traces obtained at four working-pressure settings while maintaining a 1:4 acetylene-to-oxygen (kPa) ratio: 25:100, 50:200, 75:300, and 100:400. Increasing the working pressures produced progressively greater peak overpressures. The colored traces represent measurements from the different pressure-sensor locations, and the shaded regions indicate range across repeated trials (n=3).

Table 3. Experimental Blast Output Relative to Open-Field TNT Blast Reference

Blast Parameter $PC_2H_2:PO_2$	Incident impulse (psi·ms)	Peak Overpressure (psi)
5 kg TNT at 5 m (UN Safeguard)	**23.5**	**17.7**
25:100	0.033	0.31
50:200	**26.38**	**11.96**
75:300	36.33	16.08
100:400	41.54	17.98

4 Peak Overpressure Increases Linearly with Oxy-Acetylene Loading Pressure

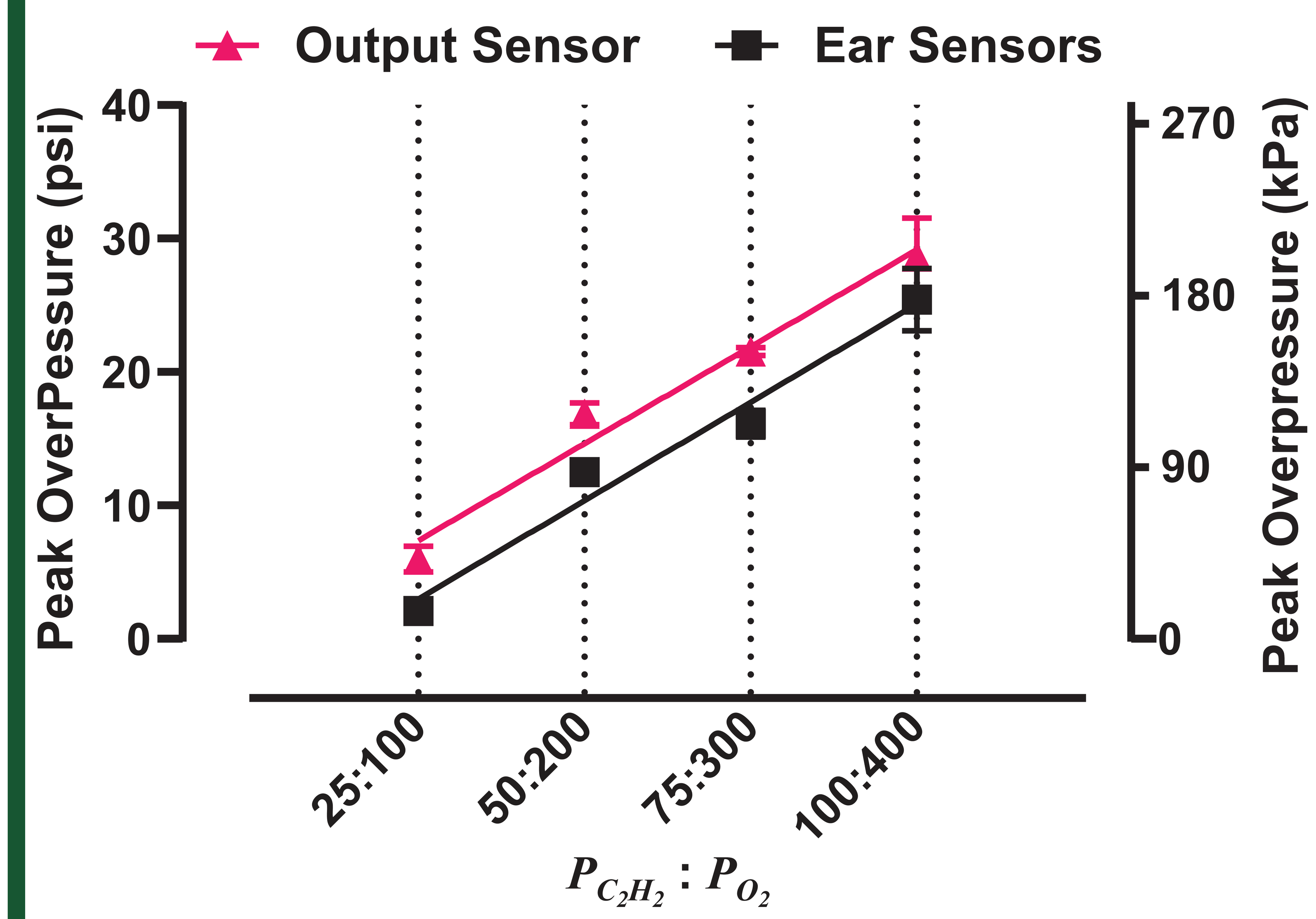

Figure 4. Peak overpressure generated across oxy-acetylene loading conditions. Peak overpressure was measured at the blast-tube output sensor and at the two sensors positioned near the ears. Acetylene and oxygen working pressures were increased proportionally while maintaining a 1:4 ratio ($P_{C_2H_2}:P_{O_2}$ = 25:100, 50:200, 75:300, and 100:400). Three independent blast trials were performed for each loading condition. Data are presented as mean ± [SEM]. Peak overpressure increased linearly with loading pressure for both the output sensor (Y=7.265X+0.096, R^2=0.906, $F_{1,10}$=96.12, $p<0.0001$) and the ear sensors (Y=7.367X −4.377, R^2=0.863, $F_{1,22}$=138.8, $p<0.0001$). The right y-axis shows the corresponding pressure in kPa.

5 Peak Overpressure Increases and Plateaus with Repeated Gas-Loading Cycles

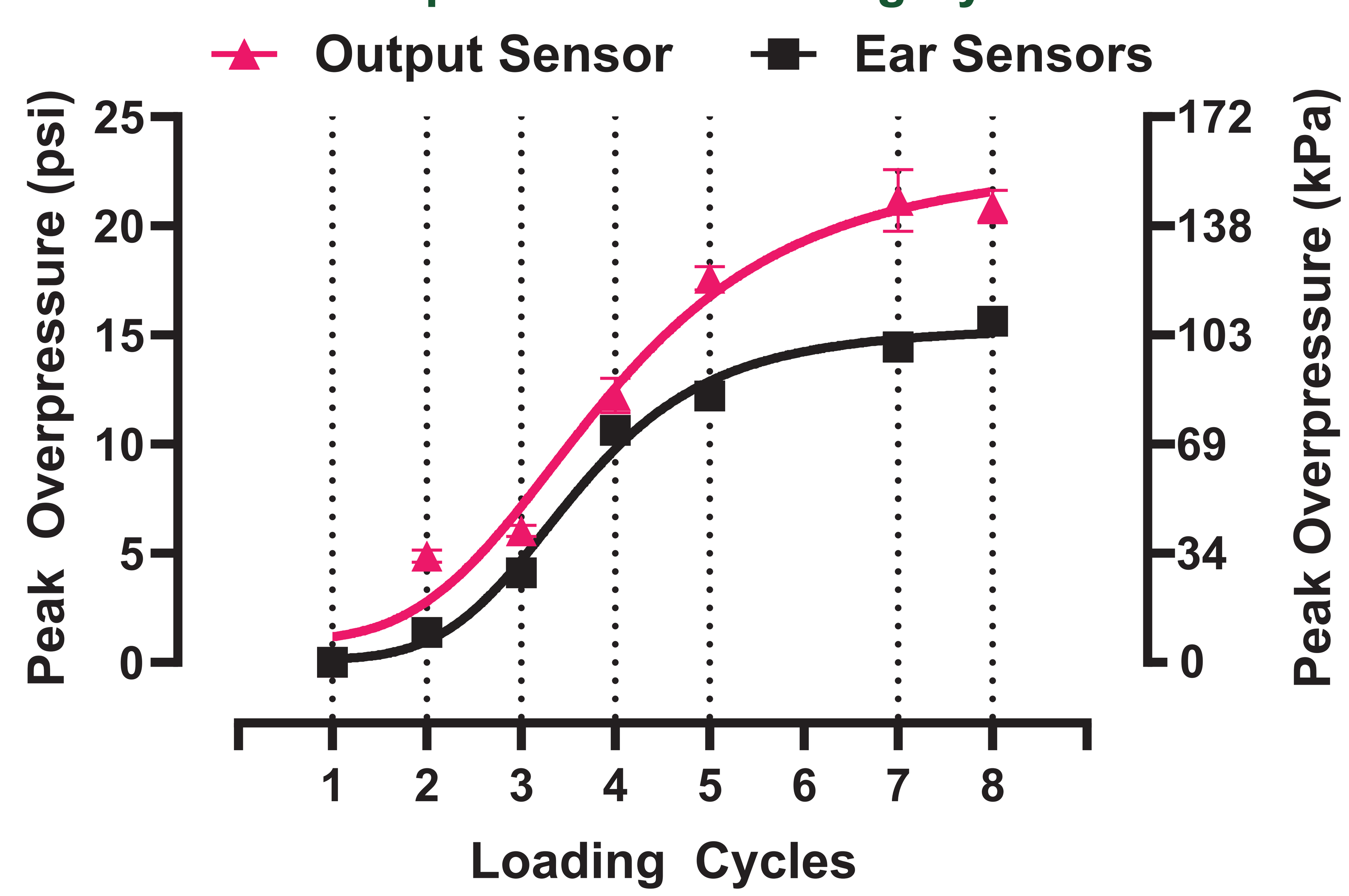

Figure 5. Relationship between gas-loading cycles and peak overpressure. Peak overpressure was measured at the blast-tube output and at sensors positioned near the ears following 1–8 oxy-acetylene loading cycles at 25:100 working pressure ratio. Data are presented as mean ± [SEM] and were fitted using a four-parameter logistic model. Peak overpressure increased sigmoidally before approaching a plateau at approximately 7–8 loading cycles. The fitted upper plateaus were 23.03 psi for the output sensor and 15.38 psi for the ear sensors, with half-maximal responses occurring at 3.89 and 3.58 loading cycles, respectively. The models showed strong goodness of fit for both the output sensor (R^2=0.940) and ear sensors (R^2=0.938). The secondary y-axis shows the corresponding pressure in kPa.

ACKNOWLEDGEMENT

National Institute on Deafness and Other Communication Disorders
Advancing the science of communication to improve lives

VA I01RX003532
NIDCD R01DC019158
DOD HT9425-23-1-0709